NPS/Int.CO 68-14
30 July, 1968

RIPPLE COMPENSATION OF THE SLOW EXTRACTED BEAM

(THEORETICAL STUDIES)

M. Conte

* * *

MPS/Int.CO 68-14
30 July, 1968

RIPPLE COMPENSATION OF THE SLOW EXTRACTED BEAM

(THEORETICAL STUDIES)

1. Introduction

The irregular profile of the time structure of the slow extracted beam is supposed to depend upon the ripples of the main (guide) field.

In fact, the guide field has ripples with frequencies of 50 Hz and 600 Hz and the same frequencies characterise roughly the irregularities of the time structure of the extracted beam.

In this note, only the 50 Hz ripple is taken into consideration, because it is capable of giving a rather complete view of the phenomenon, without involving too long computations.

The order of magnitude of this ripple is supposed to be about 10^{-6} of the actual value of the guide field.

A library program [1] has been taken over, considering a rather theoretical perturbed machine, which corresponds, more or less, to an existing model [2]. Its general features are:

6 sextupoles at straight sections (ss)

5-, 25+, 35-, 45+, 85-, 95+

(where signs + and - refer to their polarities)

6 bump coils at the bending magnet

51.5-, 58.5+, 60.5-, 61.5-, 66.5+, 67.5+

(where xy.5 refer to the bending magnet between ss xy and ss(xy+1))

1 quadrupole at ss 61 (with positive polarity).

The strengths of the above elements are, if normalized according to a chosen criterion [3] (extensively described in Appendix I):

$$K_{B.C.} = \pm 15.8$$
$$K_1 = 2.0$$
$$K_2 = \pm 0.002$$

The value of Q_R across the vacuum chamber is considered constant (equal to 6.25).

2. Effect of the guide field ripple on the stable area

The procedure of extracting the beam is outlined in a way as close to reality as possible. Namely, after having turned on all the perturbing elements, the beam is spilt out by displacing outward the closed orbit. The beam is supposed to be monoenergetic.

This spill-out may be interpreted in the phase plane, as bringing the stable area to a vanishingly small value. The radial displacement should take place steadily and over a time interval of 200 msec, corresponding roughly to the practical duration of the resonant spill.

The corresponding variation of the stable area is represented in Fig. 1. This plot is obtained by inserting into the program the values of the closed orbit, which correspond to different time moments. The broken straight line in the figure is to make evident how far the time variation of the stable area is from a linear function.

Now a radial ripple is added to the linear variation of the closed orbit. The whole variation can be described by the following simplified formula:

$$x_{c.o.}(t) = (x_{c.o.})_{t=0} + \rho t + dr(t) \qquad (1)$$

where $dr(t)$ is evaluated through the approximate general relation (see

Appendix II for its discussion):

$$\frac{dr}{r} \simeq -\alpha \frac{\delta B}{B} \qquad (2)$$

where α is the momentum compaction factor and $\delta B/B$ can be any time variation of the guide field.

At present, α is set equal to $1/Q_R^2$ and $\delta B/B$ is just the guide field ripple, outlined as a sinusoidal function with frequency of 50 Hz and with its extreme values equal to $\pm 10^{-6}$.

Bearing in mind equation (1) and what has just been discussed, several values of $x_{c.o.}$ are evaluated, spanning the whole length of the spill by time steps of 5 msec (a quarter of a period of the considered frequency) and by smaller steps (1 msec) in the middle of the spill (90 msec $\leq$ t $\leq$110 msec), by means of an ancillary program [4].

Running the main program for each value of the closed orbits so evaluated, the corresponding values of the stable area so obtained are gathered as in Fig. 2, which shows nothing but the time variation of the stable area under the effect of the guide field 50 Hz ripple.

The broken curve of Fig. 2 is the former solid curve of Fig. 1, reapeated here as a reference.

3. Construction of the time structure of the extracted beam

The results so far obtained need a few comments. In fact, once a proton is out of the stable area, it goes away to relevant distances in a matter of a few tens of turns; while the ripple-affected expansion takes place over a time interval equal to half a period of the considered ripple, i.e. 10 msec or 500 turns.

Thus it is possible to state that as long as the stable area A(t) decreases, i.e. its time derivative is negative, the extraction occurs; as soon as this derivative becomes null or positive, the extraction is immediately stopped, and this interruption lasts till the derivative becomes negative again.

After these considerations, it is at once evident that if a beam is extracted by shrinking the stable area as in Fig. 2, its time structure must look like a set of successive bursts.

This achievement may be attained in a slightly more quantitative way. In fact, if a function $\Phi(t)$ is defined as follows:

$$\Phi(t) = -\frac{dA}{dt}, \qquad \text{for } \frac{dA}{dt} < 0 \tag{2a}$$

$$\Phi(t) = 0, \qquad \text{for } \frac{dA}{dt} \geq 0 \tag{2b}$$

(where $A = A(t)$ is the stable area); it is correct to assume that this function is proportional to the flux of extracted protons (for a further discussion, see Appendix III).

Fig. 3 shows the function $\Phi(t)$ when deduced from the stable area $A(t)$ represented in Fig. 2. Indeed, the bursts of Fig. 3 are obtained by inserting into eq.(2) an approximate analytical form of $A(t)$ which fits rather well with graph of Fig. 2.

The declining shape of the bursts is due to the downward bump which affects the "unrippled" time variation of the stable area (see Fig. 1).

4. Compensation of the ripple effects

In order to reduce or to eliminate the ripple effects on the time structure of the slow ejected burst, a closed loop control has been proposed [5].

One of the main features of this method consists of the use of some kickers. At present, two kickers are employed, located respectively at ss 35 and ss 95, according to an experimental [6] setting-out.

The polarities of these two kickers are opposite and vary in time according to a sinusoidal law, showing their extreme values as follows:

$(35+)_{max}$ $(95-)_{min}$, when $t = T(\frac{1}{4} + h)$

$(35-)_{min}$ $(95+)_{max}$, when $t = T(\frac{3}{4} + h)$

where $T = 20$ msec and $h = 0, 1, 2, \ldots 9$.

The same current is supposed to be fed into the coils of both kickers [7) 8)] but in opposite polarities. The corresponding normalized (see again Appendix I) strengths are introduced into the main program [1)], always bearing in mind the proper value of the closed orbit corresponding to each time moment.

Both currents should be zero at the instants which correspond to the crossing points between the broken curve and the solid curve of Fig. 2, i.e. when $t = \frac{T}{2} h$, with $h = 0, 1, 2, \ldots 20$. In fact, both curves being coincident at these instants, no compensation is needed.

The subsequent result consists of compensating the sinusoidal bumps of Fig. 2, to the encircled points of Fig. 4, by feeding a "theoretical" current of 2.0 mA (found by inspections).

These points are compared with the function $A(t)$ in absence of ripple (solid curve of Fig. 1 repeated in Fig. 4), and nearly no differences are noticeable.

Finally, if the criterion discussed in chapter 3 and Appendix III is now applied, a continuous* burst, shaped as in Fig. 5, is found.

---

* A wish of the author would be to normalize the arbitrary units used in Fig. 3 and Fig. 5 in such a way that the area, contained by the set of peaked bursts of Fig. 3 has to be equal (same amount of protons spilt out) to the area contained by the continuous burst of Fig. 5. Anyway, it is suggested that the reader bear in mind this normalization.

5. Comments

A few more cases with various momentum spreads should be computed, but it may be guessed that the final response should not be too different from the results so far obtained. Only, it might happen that for some value $\Delta p/p$ (possibly for a negative $\Delta p/p$), the slope of the stable area is steeper than the one shown in Fig. 2, i.e. the gap between two successive bursts becomes narrower (Appendix III).

Moreover, if the momentum distribution is supposed gaussian (Fig. 6), the burst of Fig. 3, which was regarding a monoenergetic beam, can still be referred to a more physical beam, i.e. with a quite realistic momentum spread.

Once at this stage, it is suggested to try to outline a completely more realistic model, i.e. with $Q_R = Q_R(x)$, measured closed orbit values, actual currents in the various perturbing elements, a spill-out commencing when the stable area has a value corresponding to the measured one and, of course, realistic momentum distribution.

It is advisable to give a further look at the effects of the 600 Hz ripple, at least over a complete cycle, using the above procedure. A further fine structure of the bursts of Fig. 3 is expected.

6. Conclusions

The compensating current found by computation is definitely too small, if compared with the actual values used in practice. In fact, the latter is of the order of 150 mA.

A reason for this discrepancy is certainly given by an initial (beginning of the spill) value of the stable area, which is far smaller than the measured one. In fact, considering that the guide field ripple and the stable area variations are in fixed proportions, for a given ripple a smaller stable area results in smaller variations to be compensated.

A further reason can be the actual value of the guide field ripple; i.e. instead of being exactly 10^{-6}, as has been considered in this note, it is very possibly bigger by a factor greater than one.

In conclusion, it can be guessed that a more realistic model should yield more reliable values for the compensating currents. Nevertheless, although this situation exists, the principle of the guide field ripple effects and compensations has been conclusively demonstrated.

The profile of the extracted beam found by computations (Fig. 5) is steeper than that actually measured [6], as it is clear looking at Fig. 7 (allowances must be made for background noise).

This difference can be explained by considering the actual way of operating the used program[1]. In fact, this program considers the phase plane distribution of the circulating protons as being uniform, while in reality this distribution fits with a gaussian law [9) 10)]. After selecting a method of shrinking the stable area, the spill-out progresses and more protons are involved, due to their crowding towards the centre of the stable area. Thus, the theoretical slope of the ejected burst is lifted, in reality, by this higher central distribution of protons.

In this case, a more realistic model should not help too much in fitting computations with measured values, even though it had to yield a stable area less curved than that of Fig. 1.

As final conclusion, it is repeated and emphasized that the irregularities of the time structure of the ejected burst are due to the ripple (s) of the guide field. As the slope at the flat-top is the driving term for the process of the resonant extraction, it may be stated that the ripple affecting this driving term is mainly responsible for these irregularities, and this should be true for any driving term taken into consideration. One example is so far known [11] where the driving term is given by a slow variation of the field index of a weak focusing synchrotron. This variation is obtained by feeding a current into a few wires of a system of pole-face windings. Now, the same ripple affecting this current is very well recognized as a signal coming from a counter struck by the resonant expanding beam.

Acknowledgements

Thanks are due to D. Dekkers and L. Henny for general information on the CPS and its deails.

Thanks are also due to E.J.N. Wilson (ISR Division) for discussions on the matter treated in Appendix III.

The author is particularly indebted to G. Shering and S. Summerhill for discussions and information on the actual subject of this note.

M. Conte

Distribution

A. Asner
Y. Baconnier
O. Bloess
C. Bovet
G. Brianti
O. Barbalat
D. Dekkers
L. Henny
H.G. Hereward
L. Hoffmann
Ch. Iselin
R. Gouiran
M. Georgijevic
J.H.B. Madsen
G. Plass
K.H. Reich
G. Rosset
P.H. Standley
Ch. Steinbach
S. Summerhill
P. Strolin
E.J.N. Wilson

E.i.C.'s

REFERENCES

1) P. Strolin, Note on the Use of the FORTRAN Program PRTAGS, CERN 6600 Computer, Program Library, Long write-up T 301 (1967)

2) C. Bovet, Variation des paramètres de l'éjection lente MPS/DL Int. 65-6 (1965)

3) C. Bovet, Programmes FORTRAN CERN pour le calcul des trajectoires perturbées et des systèmes d'éjection par resonance dans le CPS MPS/Int.DL 65-5 (1965)

4) M. Conte, FORTRAN Program DAPELP (1968)

5) G. Shering and S. Summerhill, Slow Ejection Burst Control (Preliminary report), MPS/CO Note 67-18 (1967)

6) S. Summerhill, private communication

7) J.J. Merminod and W. Richter, The Use of the Kicker Magnets in the PS, MPS/Int/VA 61-6 (1961)

8) J. Guillet, Mesure de la répartition du champs dans l'entrefer d'un dipole du PS, MPS/SR/Note/68-18 (1968

9) C. Bovet et C. Guignard, Mesure de l'emittance d'un faisceau primaire SI/Note DL/68-7 (1968)

10) M. Conte, Resonant Extraction from an Ideal Circular Weak Focusing Synchrotron, Nucl.Instr.Methods., 62, 269 (1968)

11) N.M. King, private communication
(The circulating beam of Nimrod, the British 7 GeV proton synchrotron, is brought up to resonance by a second harmonic sextupolar perturbation. A big share of the beam succeeds in entering into the mouth of a septum magnet, being thus driven against an internal counter.)

APPENDIX I

NORMALIZATION OF THE PERTURBING STRENGTHS

The general expression for the normalized strength of any lens of order n is:

$$K_n = 12.0 \times N^{n+1} \frac{\Delta x'(\text{mrad})}{x^n(\text{mm})} \qquad \text{I.1)}$$

where:

$N = 1$ in the F (even) straight sections,

$N = \sqrt{\frac{\beta_F}{\beta_D}} \simeq 1.35$ in the D (odd) straight sections

$N = \sqrt{\frac{\beta_M}{\beta_D}} = \sqrt{\frac{\beta_F}{\beta_M}} \simeq 1.16$ in the middle of a magnet;

$n = 0$, for kickers and bump coils

$n = 1$, for quadrupoles

$n = 2$, for sextupoles.

The quantity $\Delta x'$ in eq. (I.1) is assessed as follows:

$$\Delta x' = \frac{L}{B_o r_o} b(x) \qquad \text{(I.2)}$$

where:

L = length of the lens

$B_o r_o$ = beam magnetic rigidity

$b(x)$ = lens magnetic induction.

The latter quantity can take the following values:

$b(x) = G_o$, for kickers and bump coils

$b(x) = G_1 x$, for quadrupoles

$b(x) = G_2 x$, for sextupoles.

Furthermore, $G_o = g_o I_o$, $G_1 = g_1 I_1$ and $G_2 = g_2 I_2$, where I_o, I_1 and I_2 are the currents fed into the respective lenses. The values of g_o, g_1 and g_2 are, if the lengths of all the lenses are set equal to 1 metre:

$g_o \simeq 18$ Gs/Amp, for kickers

$g_o = 4.2$ Gs/Amp, for bump coils

$g_1 = 0.425$ (Gs/cm)/Amp, for quadrupoles

$g_2 = 0.25$ (Gs/cm^2)/Amp, for sextupoles.

APPENDIX II

CLOSED ORBIT DISPLACEMENT DUE TO A TIME VARIATION OF THE GUIDE FIELD

The effect of a slight time variation (δB) of the guide field on the circulating beam, at constant energy, consists of altering the equilibrium orbit radius by an amount obtainable from the following relation:

$$B\,dr + r\left(\delta B + \frac{dB}{dr}\,dr\right) = 0 \qquad \text{(II.1)}$$

where the first term in the bracket corresponds just to the effect of interest while the second term indicates how the value of the guide field is changed by the radial displacement dr. (It is the way of writing (II.1) which is rather approximate.)

From eq. (II.1) the following expression is deduced:

$$\frac{\delta B}{B} = -\left(1 + \frac{r}{B}\frac{dB}{r}\right)\frac{dr}{r} \qquad \text{(II.2)}$$

recalling the fundamental relation

$$\frac{dp}{p} = \frac{1}{\alpha}\frac{dr}{r} \qquad \text{(II.3)}$$

with α = momentum compaction factor and remembering that

$$\frac{dp}{p} = \frac{dr}{r} + \frac{dB}{B} \qquad \text{II.4)}$$

Cancelling $\frac{dp}{p}$ between (II.3) and (II.4):

$$1 + \frac{r}{B}\frac{dB}{dr} = \frac{1}{\alpha}$$

which inserted into (II.2) gives just the relation (2) of Sect. 2.

APPENDIX III

TIME SHAPE OF THE EJECTED BEAM FROM TIME VARIATIONS OF THE STABLE AREA

Let us proceed by successive examples, in order to be as concise as possible.

a) A steadily shrinking stable area

$$A(t) = A_o - at$$

gives a constant burst (φ_o), if the protons are supposed to have a uniform phase plane distribution. The shorter the duration of this burst, the bigger the number of extracted protons per time unit. But a shorter burst means, keeping A_o unaltered, a steeper slope of A(t), i.e. a higher absolute value of its derivative. In conclusion, φ_o is proportional to $-\frac{dA}{dt}$, as stated in Sect. 3.

b) A downward bumped stable area variation

$$A(t) = A_o e^{-(t/\tau)} - a't$$

yields, applying what was discussed before:

$$\varphi(t) = a' + \frac{A_o}{\tau} e^{-(t/\tau)}$$

i.e. a burst with a declining shape (similar to that of Fig. 5).

c) A ripple is added to the steady variation:

$$A(t) = A_o - at - e \sin \omega t$$

Bearing in mind what was discussed in Sect. 3 and at point a):

$$\varphi(t) = 0 \qquad \text{for } \frac{dA}{dt} = -a - \omega e \cos \omega t \geq 0$$

$$\varphi(t) = a + e \cos \omega t, \text{ for } \frac{dA}{dt} = -a - \omega e \cos \omega t < 0$$

i.e. the former continuous burst is split into a set of peaked bursts, of which each couple is separated by a time gap

$$\delta t = \frac{T}{2} - \frac{a}{\omega^2 e}$$

with T equal to the ripple period.

The latter formula, valid indeed for a shrinking law different from the computed one, still gives reliable information on how this time gap depends upon a (stable area slope) and upon ω (ripple frequency).

Clearly, the bigger a, the narrower δt and, consequently, the thicker the bursts (beginning of Sect. 5). And, the higher ω the wider δt (end of Sect. 5) and more peaked the bursts (footnote on page 5).

d) The function best fitting the computed plot of Fig. 2 is:

$$A(t) = A_o e^{-\frac{t}{\tau}} - a't - \Sigma\omega \sin \omega t$$

which was plotted by means of the ancillary program mentioned in Sect. 2. (A_o, Σ and ω are directly given, τ and a' are compiled by the program itself, through two given values of $A(t)$: A(final and A(middle)).

Fig. 1

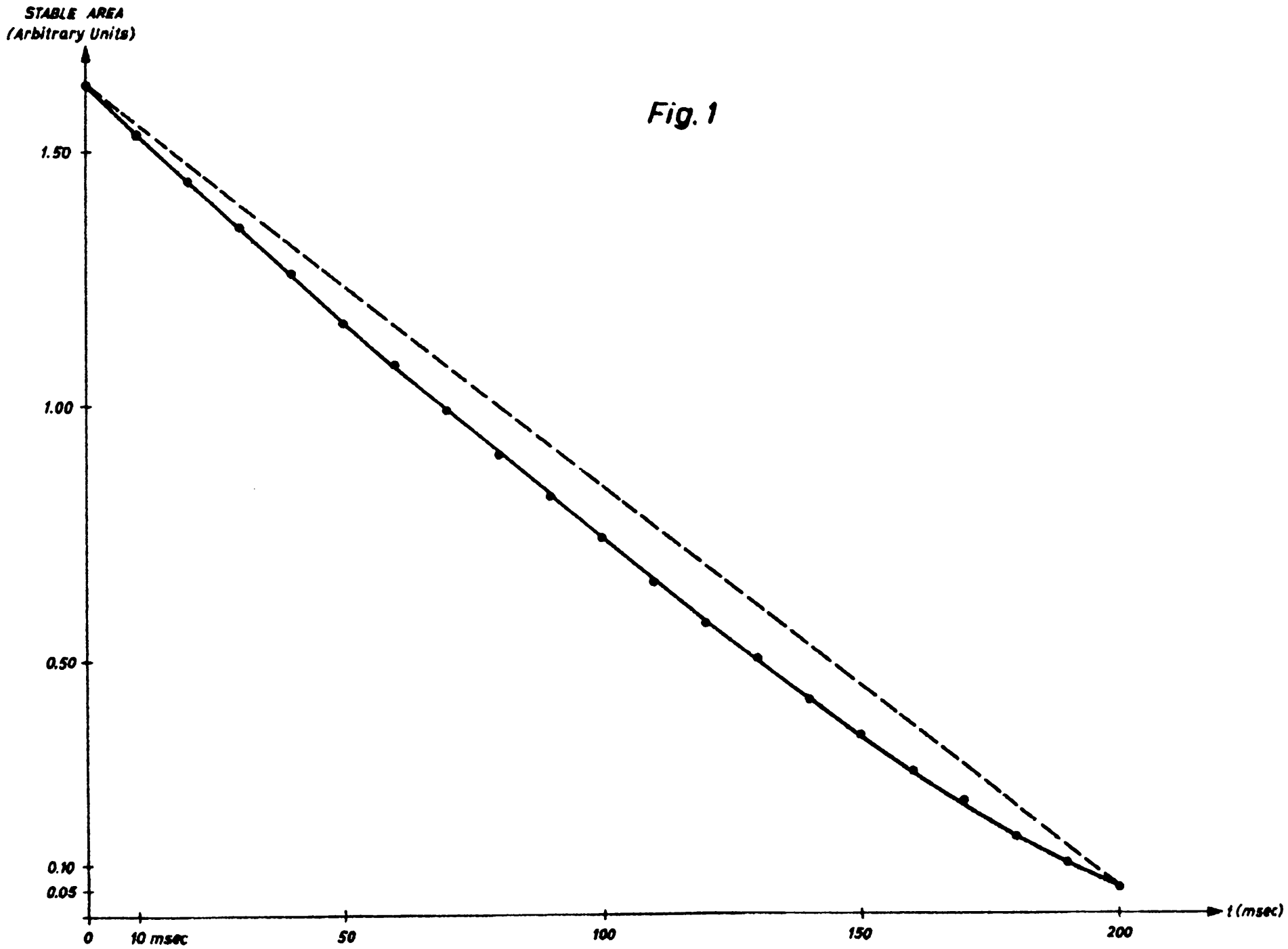
STABLE AREA
(Arbitrary Units)
1.50
1.00
0.50
0.10
0.05
0
10 msec
50
100
150
200
t (msec)

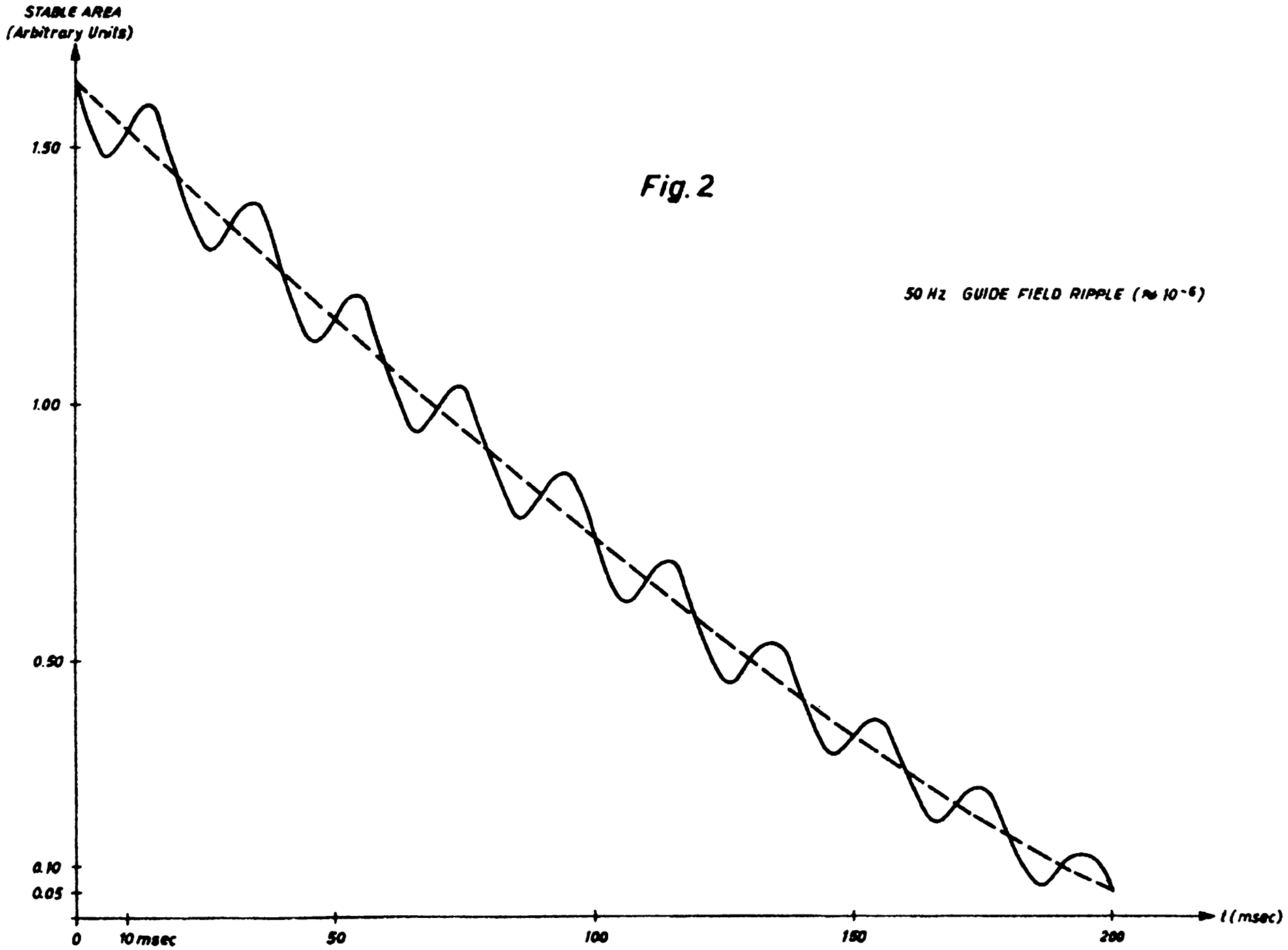
STABLE AREA
(Arbitrary Units)
1.50
1.00
0.50
0.10
0.05
0
10 msec
50
100
150
200
t (msec)
50 Hz GUIDE FIELD RIPPLE (≈ 10⁻⁶)

Fig. 2

Fig. 3

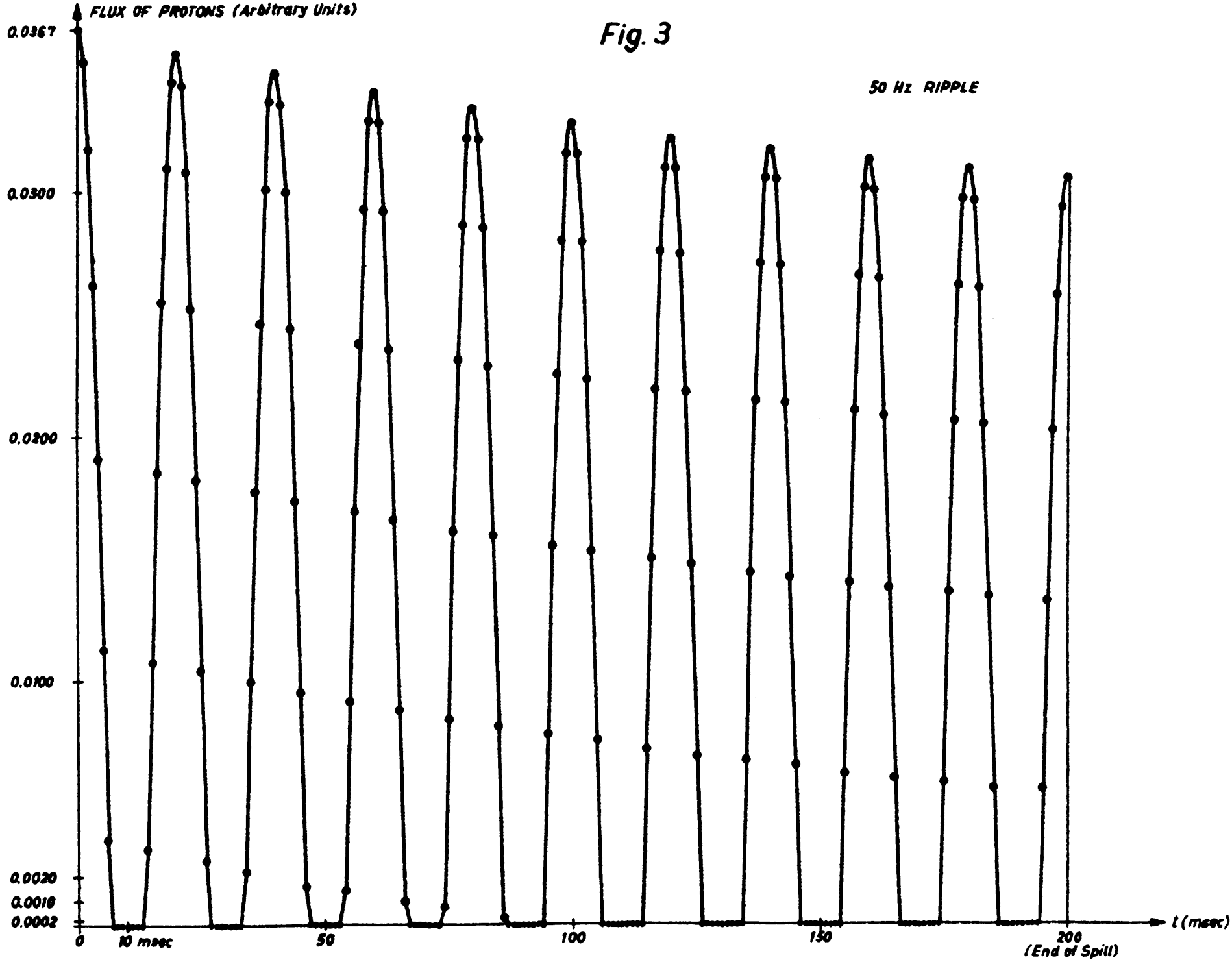
FLUX OF PROTONS (Arbitrary Units)
50 Hz RIPPLE
0.0367
0.0300
0.0200
0.0100
0.0020
0.0018
0.0002
0
10 msec
50
100
150
200
(End of Spill)
t (msec)

Fig. 4

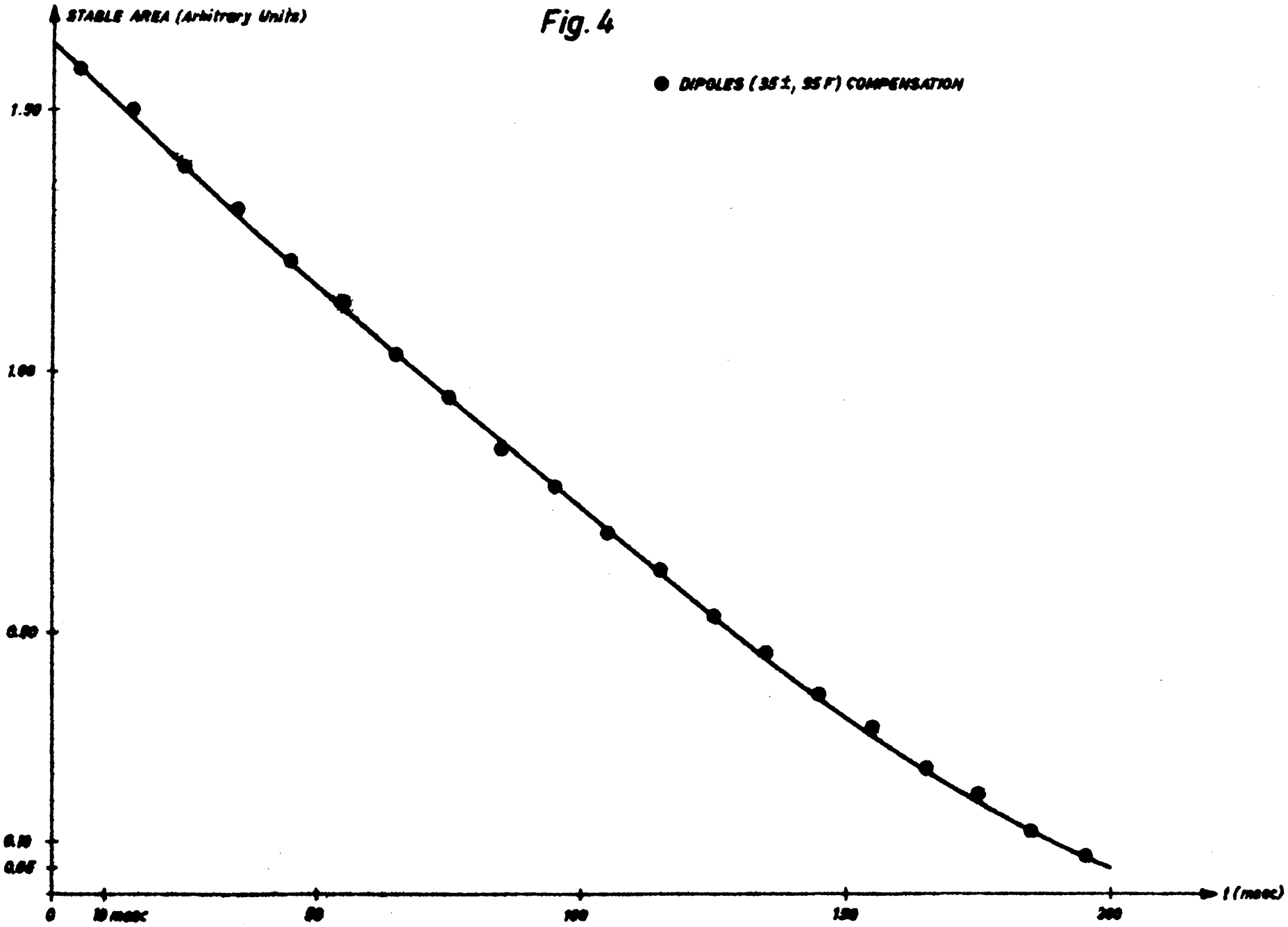
STABLE AREA (Arbitrary Units)
DIPOLES (35 Å, 55 F) COMPENSATION
1.50
1.00
0.50
0.10
0.05
0
10 msec
50
100
150
200
t (msec)

Fig. 5

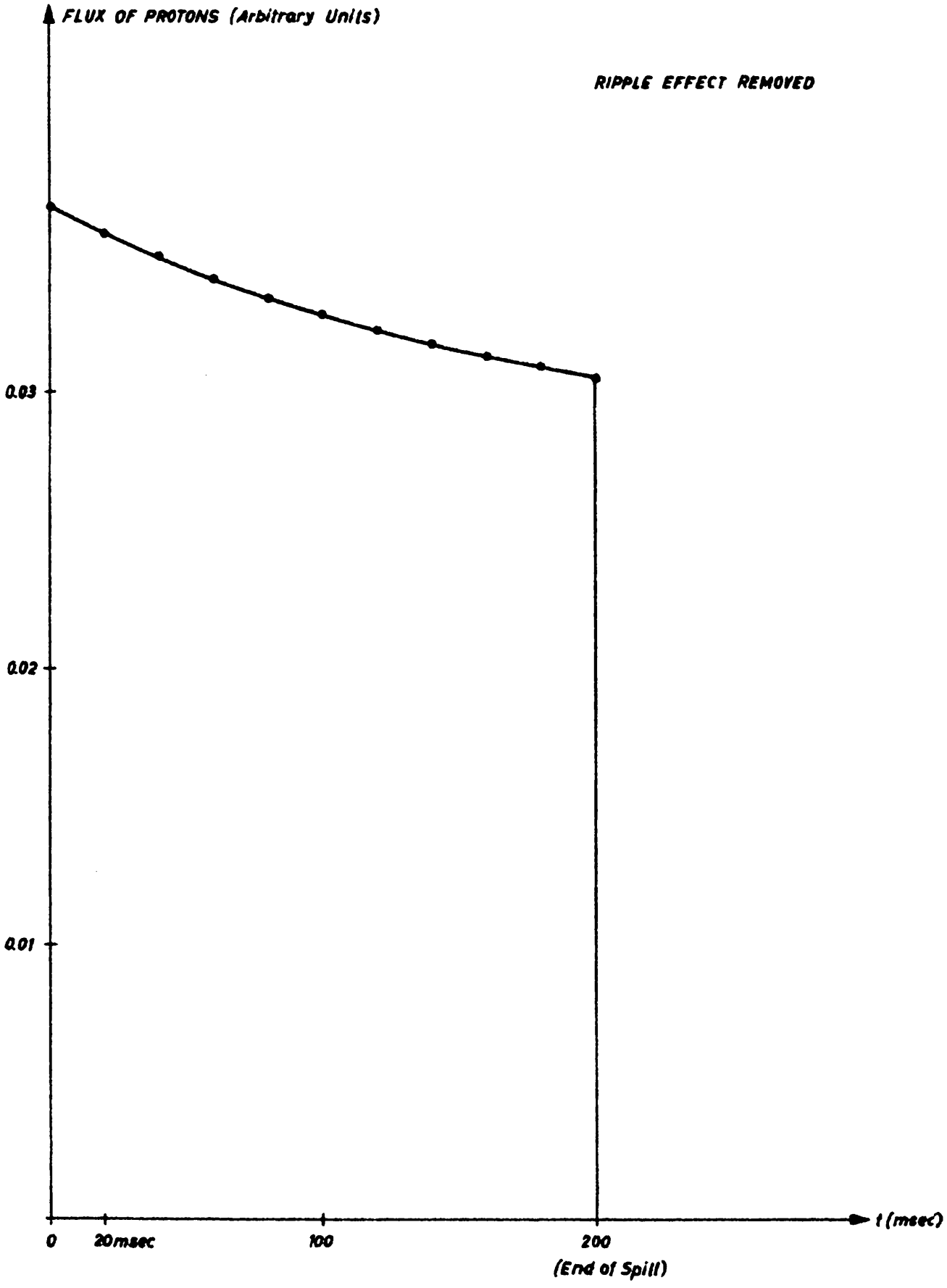
FLUX OF PROTONS (Arbitrary Units)
RIPPLE EFFECT REMOVED
0.03
0.02
0.01
0
20msec
100
200
(End of Spill)
t (msec)

Fig. 6

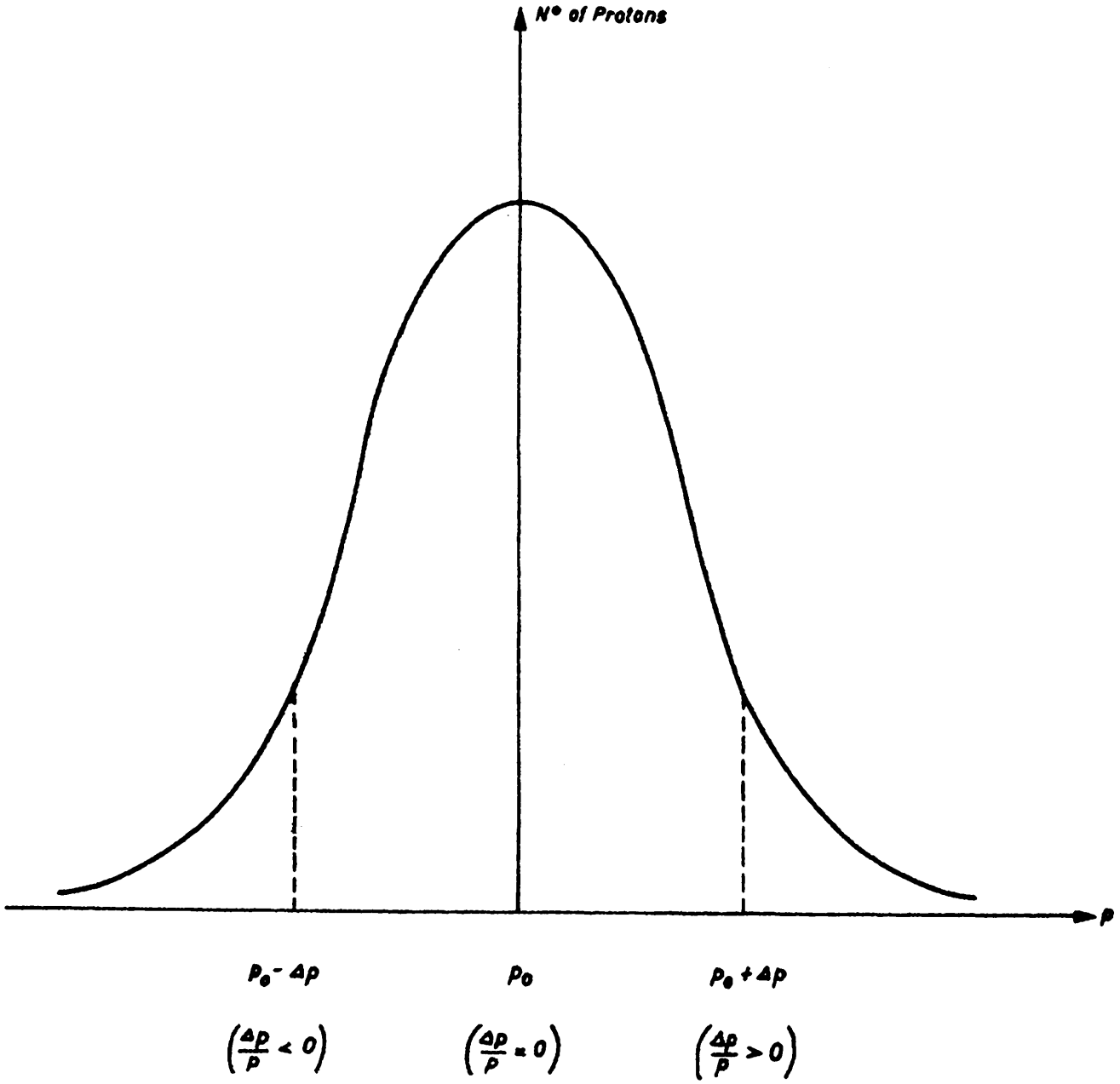
N° of Protons
p
$p_0 - \Delta p$
p_0
$p_0 + \Delta p$
$\left(\frac{\Delta p}{p} < 0\right)$
$\left(\frac{\Delta p}{p} = 0\right)$
$\left(\frac{\Delta p}{p} > 0\right)$

Fig. 7

COMPENSATED EJECTED BURST

(Picture dated 25 th may 1968)